

Design of a Microstrip-Fed Printed-Slot Antenna Using Defected Ground Structures for Multiband Applications

Nasr H. Gad^{1,2} and Matjaz Vidmar¹

¹Radiation and Optics Laboratory, Faculty of Electrical Engineering
University of Ljubljana, Ljubljana 1000, Slovenia
nasr.gad@fe.uni-lj.uni.si, matjaz.vidmar@fe.uni-lj.uni.si

²Physics Department, Faculty of Science
Ain Shams University, Cairo 11566, Egypt
ngad@sci.asu.edu.eg

Abstract — This paper presents the design of a microstrip-fed, planar-printed, slot antenna using defected ground structures (DGSs) for multiband applications. The antenna structure consists of two groups of five straight slot elements. The slot elements in each group are of the same width but different lengths on the ground plane and separated by a small strip and a slot cut on both sides of the strip to interconnect the group of slots with each other. The microstrip line is designed on the front side of the PCB with a right angle for all the slots to make it easy to mount the slots and the microstrip with a monolithic microwave integrated circuit (MMIC). The proposed antenna is designed and simulated using an electromagnetic simulator based on the method of moment (MoM). For the validation the antenna was fabricated on a double-sided substrate material that was 0.79 mm thick with an area of 45 × 40 mm². The simulation and measurement results show that the antenna has good input-impedance bandwidths of $S_{11} \leq -10$ dB at the five operating frequencies of 3.5, 4.1, 5, 6.4, and 6.8 GHz and that extends in the range 2 to 7.5 GHz. The measurements were found to be in good agreement with the simulation results for S_{11} and provide a stable radiation pattern.

Index Terms — Defected ground structure (DGS), microstrip line, multiband applications, printed slot antenna.

I. INTRODUCTION

The rapid growth in wireless communications means everything around us is being upgraded to wireless and the need for planar printed antennas has increased in recent years. The printed-slot antenna is one type of printed antenna that has been investigated extensively for several decades because of its attractive features, light weight, low profile, compactness and because it easy to integrate with other circuits. Its multiband

characteristics make it the most suitable choice for modern wireless-communication systems.

The interests of researchers in studying planar, printed-slot antennas with a microstrip line can be seen in the literature for dual-band applications [1-4]. The design of a dual-frequency band using different stub configurations has increased the whole area of the antenna and controlled the frequency bands [5]. Many researchers have been concerned about the design of printed antennas in the area of tri-band [6-8] and quad-band [9-11] applications. A defected ground structure (DGS) is realized by etching the slots or defects on the ground plane under the microstrip line. DGSs with broad cell shapes have been studied with respect to designing microwave circuits such as filters and antennas [12, 13]. In [9], a microstrip-fed right-angle slot antenna with different lengths for quad-band applications with an end offset feed is presented. In [10], a four-band microstrip fed slot antenna is proposed based on the rectangular slot in the ground plane and by adding T- and E-shaped stubs to produce four frequency bands. In the work reported in [11], a microstrip line with a right-angle-fed, rectangular, wide-slot antenna is developed for quad-band applications.

In this paper the study of a planar-printed slot antenna with a microstrip line feeder for multiband applications is presented. The proposed antenna is designed and fabricated based on a Taconic (TLT-9) substrate of 45 mm × 40 mm. Five slots with a narrow rectangular shape are etched on the ground plane as the DGS cells. The centers of all the slots are filled with a 0.5-mm strip divided into two groups of slots: right and left. The left group of slots is longer than the right group by 0.5 mm, having a cut of two slots with a 1-mm width around the strip to connect each group of slots together. The proposed printed-slot antenna is simulated and designed using an electromagnetic simulator program based on MoM to visualize the simulation results, which show the five bandwidths around the operating

frequencies of 3.5, 4.1, 5, 6.4, and 6.8 GHz. By adjusting the length of the left group of the DGS slots to be smaller than the right group by 0.5 mm, another group of operating frequencies with the bandwidths is created with 3.6, 4.2, 5.2, 6.8, and 7.3 GHz. On the other hand, by moving the strips between the two groups of slots far from the central strip and the microstrip line the wide bandwidth is obtained around the operating frequency of 5.5 GHz with a 1.666-GHz bandwidth. The proposed antenna design is based on DGS rectangular cells (narrow slots) and a microstrip line, without the need for other stubs [9, 10] or modifying the microstrip line structure with an L shape [8, 11], and not based on large aperture slots [10, 11]. The proposed antenna and the antenna with the left group of slots smaller than the right group by 0.5 mm are suitable for the long-term evolution (LTE) band 42 (3.4-3.6 GHz), band 43 (3.6-3.8 GHz), band 48 (3.55-3.7 GHz), while intelligent transportation systems (ITSs) is the technology that can provide the variety of service in the future and the C-band applications.

II. ANTENNA DESIGN

The geometry of the proposed planar printed-slot antenna is shown in Fig. 1. The slot antenna is printed on a double-sided Taconic (TLT-9) substrate with a dielectric constant $\epsilon_r = 2.55$, a loss tangent $\tan(\delta) = 0.0018$ and substrate height $h = 0.79$ mm with a copper cladding of thickness $t = 0.035$ mm on both sides of the PCB. All the antenna dimensions are designed on a total surface area of 45×40 mm². On the front side of the substrate, a microstrip line feeder with 50Ω and fixed width ($W_f = 2.2$ mm) and feeding length ($L_f = 31$ mm) are designed.

The ground plane of the proposed antenna consists of two groups of five straight slots extended horizontally with different lengths. The two groups of slots are separated by a 0.5×8.25 mm² strip with a right angle for all the slots and fills the slot area parallel to the microstrip line in a symmetrical position around the origin of the x-axis. The left group of the slots are shifted by 0.5 mm to the left due to the microstrip line view of the antenna. On both sides around this strip, there is a cut spaced with a slot width ($S = 1$ mm) and all the slots are connected together for each group of slots.

The two groups of five slots are positioned around the strip. The right and left designed groups of slots on the ground plane are created with the following lengths for the right group, L_{s1r} , L_{s2r} , L_{s3r} , L_{s4r} , and L_{s5r} , and for the left group with lengths L_{s1l} , L_{s2l} , L_{s3l} , L_{s4l} , and L_{s5l} , and a fixed width ($S = 1$ mm) for all the slots. The separation between the slots controls the impedance bandwidth of the antenna, the separation between slots is fixed with ($S_1 = S_2 = S_4 = 0.75$ mm) and the only different separation is ($S_3 = 1$ mm) between L_{s3} and L_{s2} for both groups, left and right (as shown in Fig. 1 (b)), and with the length ($L_m = 0.75$ mm) between the open end of the microstrip line and the smallest slots (L_{s1r} and

L_{s1l}) for adjusting the impedance (as shown in Fig. 1 (a)).

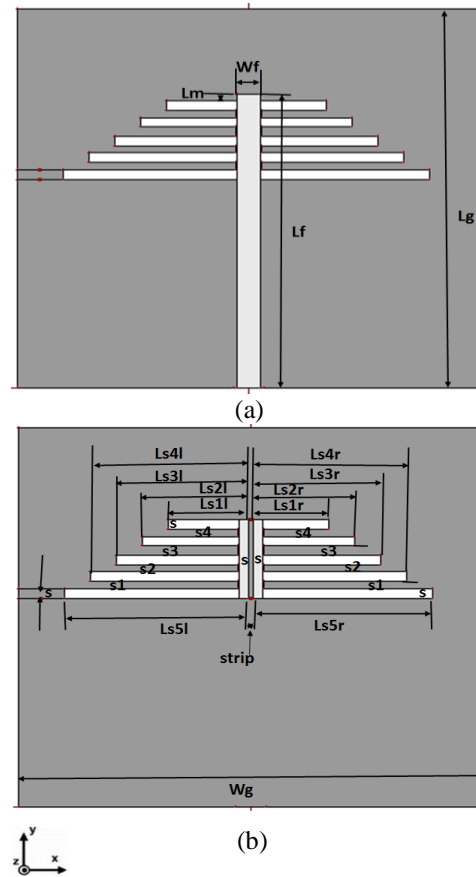


Fig. 1. Geometrical layout of the proposed planar printed slot antenna: (a) top layer and (b) bottom layer.

All the parameters for the proposed antenna are shown in Table 1.

Table 1: Dimensions of all the elements of the proposed antenna

Parameter	Size (mm)	Parameter	Size (mm)	Parameter	Size (mm)
W_g	45	L_{s1r}	7.25	L_{s1l}	7.75
L_g	40	L_{s2r}	9.75	L_{s2l}	10.25
W_f	2.2	L_{s3r}	12.25	L_{s3l}	12.75
L_f	31	L_{s4l}	15.25	L_{s4r}	14.75
L_m	0.75	L_{s5l}	17.75	L_{s5r}	17.25
S	1	S_1	0.75	S_2	0.75
S_3	1	S_4	0.75	strip	0.5

In order to achieve multiband operation for the printed-slot antenna, the slot length of each radiating element must be around $\lambda_g/2$ [14]. The slot antenna length is referred to the guide wavelength λ_g , which is given by:

$$\lambda_g = \frac{c}{f \sqrt{\epsilon_e}}, \quad (1)$$

where ϵ_e is the effective dielectric constant:

$$\epsilon_e \approx \frac{(\epsilon_r + 1)}{2}, \quad (2)$$

The slots ($Ls5r + Ls4r + S1$) and ($Ls5l + Ls4l + S1$) produce the bandwidth around the operating frequency for 3.5 GHz, ($Ls4r + Ls3r + S2$) and ($Ls4l + Ls3l + S2$) produce the bandwidth around the operating frequency for 4.1 GHz, ($Ls3r + Ls2r + S3$) and ($Ls3l + Ls2l + S3$) produce the bandwidth around the operating frequency for 5 GHz, ($Ls2l + Ls1l + S4$) produce the operating frequency for 6.4 GHz and finally ($Ls2r + Ls1r + S4$) produce the operating frequency for 6.8 GHz. All the radiating elements are shaped like an unequal U-slot as the DGS cell. The shortest slots are the active radiators and the longest slots are to improve the impedance matching for the first three operating frequencies (3.5, 4.1, and 5 GHz). Table 2 shows all the operating frequencies with the radiating slot length.

Table 2: Radiating slot length for all the operating frequencies

Freq./ λ_g (mm)	Length of the Radiating Slot Right Group	Length of the Radiating Slot Left Group
3.5GHz/ 59.04	$Ls5r + Ls4r + S1 =$ 32.75 mm = $0.55\lambda_g$	$Ls5l + Ls4l + S1 =$ 33.75mm = $0.57\lambda_g$
4.1GHz/ 50.4	$Ls4r + Ls3r + S2 =$ 27.75 mm = $0.55\lambda_g$	$Ls4l + Ls3l + S2 =$ 28.75 mm = $0.57\lambda_g$
5GHz/4 1.33	$Ls3r + Ls2r + S3 =$ 23 mm = $0.556\lambda_g$	$Ls3l + Ls2l + S3 =$ 24 mm = $0.58\lambda_g$
6.4GHz/ 32.29		$Ls2l + Ls1l + S4 =$ 18.75 mm = $0.58\lambda_g$
6.8GHz/ 30.39	$Ls2r + Ls1r + S4 =$ 17.75 mm = $0.58\lambda_g$	

By changing the slot lengths of the left group of the proposed antenna without changing the slot lengths of the right group, shown in Table 3, a comparison is made between the proposed antenna and other three different antennas (antenna 1, antenna 2, and antenna 3) for the simulated return loss shown in Fig. 4.

All the left group of slots in antenna 1 equal the right one, and for antenna 2 all the left slots are shorter than the same group in the proposed antenna by 1 mm and the other five operating frequencies with their bandwidths are obtained. For antenna 3 all the left slots are longer than the same group in the proposed antenna by 0.5 mm, and the other eight operating frequencies with their bandwidths are created. By shifting the strips between the slots in the proposed antenna on both sides of the central strip, the wideband slot antenna is obtained with an operating frequency at 5.5 GHz with a radiating length $Ls5l = 17.75$ mm, with $\lambda_g = 37.57$ mm leading to $Ls5l = 0.47 \lambda_g$. It is also calculated for $Ls5r = 17.25$ mm,

leading to $Ls5r = 0.46 \lambda_g$. Figure 4 shows S_{11} for all the antenna configurations.

Table 3: Three antennas based on different lengths of left slots for the proposed antenna (PA)

Antenna Name	Left Slots (mm)				
	Ls1l	Ls2l	Ls3l	Ls4l	Ls5l
PA	7.75	10.25	12.75	15.25	17.75
Antenna 1	7.25	9.75	12.25	14.75	17.25
Antenna 2	6.75	9.25	11.75	14.25	16.75
Antenna 3	8.25	10.75	13.25	15.75	18.25

III. RESULTS AND DISCUSSION

The proposed planar-printed slot antennas were designed and simulated using the IE3D electromagnetic simulator software based on the method of moments (MoM). The simulated results, including the current distribution, return losses, gains, efficiency, and radiation patterns are numerically derived using the IE3D commercial software. In the IE3D software the larger the number of cells per wavelength, the better the accuracy of the simulation. However, increasing the number of cells increases the total simulation time and the memory required for simulating the structure. In many simulations, using 20 to 30 cells per wavelength should provide enough accuracy. All the parameters that affect the antenna's performance were simulated based on the method of moments. The simulated proposed antenna was printed and fabricated on double-sided metallic layers on a TLT-9 substrate.

To verify the obtained results from the electromagnetic simulator program, the structure is fabricated using the laser-based PCB prototyping LPKF protoLaser S4 and the fabricated antenna's important parameters are measured. To validate the predicted performance of this proposed slot antenna, a prototype antenna was then fabricated and measured. Figure 2 shows the photographs of the top and bottom sides of the fabricated antenna.



Fig. 2. Fabricated prototype of the proposed planar printed slot antenna: (a) top side and (b) bottom side.

Measurements on the fabricated antenna were carried out using a Rohde & Schwarz ZVA67 Vector Network Analyzer for measuring the return loss (S_{11}) and an anechoic chamber for the radiation-pattern measurements.

The detailed results are provided in the following for a comparative study.

The current distributions of the proposed antenna for the five resonant frequencies and the wideband antenna for the resonant frequency of 5.5 GHz are shown in Fig. 3.

Figure 3 shows how the current distribution affects the different parts of the proposed printed-slot antenna, depending on the frequency level (max. E-current = 26.59 (A/m)). When it reaches 3.5 GHz, the current distribution is concentrated in between the largest slots (Ls5l, Ls4l) and (Ls5r, Ls4r) with a straight shape. At a frequency of 6.4 GHz the current distribution concentrated in between the slots (Ls2l, Ls1l), and when the frequency reaches 6.8 GHz, the current distribution concentrated in the smallest slots (Ls2r, Ls1r). By moving the horizontal strips between the slots a wideband antenna is obtained with a bandwidth around 5.5 GHz (max. E-current = 22.972 (A/m)).

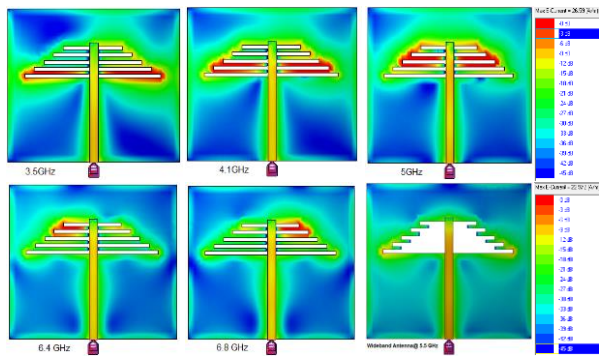


Fig. 3. Current distribution of the proposed antenna and the wideband antenna at the operating frequencies.

The return loss for all the antenna configurations is shown in Fig. 4. The simulated and measured return loss (S_{11}) of the proposed designed antenna is depicted in Fig. 4 (a). The results show good agreement with each other for all the operating bands in the range 2–7.5 GHz. The measured impedance bandwidths achieved are 3.295–3.542 GHz with a bandwidth of 0.247 GHz (7.23%), 3.893–4.156 GHz with bandwidth of 0.263 GHz (6.53%), 4.708–5.052 GHz with a bandwidth of 0.344 GHz (7.05%), and two integrated bandwidths around 6.656 GHz with ($S_{11} = -15.2$ dB) in the range of 5.789–6.656 GHz with a bandwidth of 0.867 GHz (13.93%), 6.656–7.035 GHz with a bandwidth of 0.379 GHz (5.54%), and the last two bands are considered as a wideband of 5.789–7.035 GHz with a bandwidth of 1.246 GHz (19.43%) for $|S_{11}| < -10$ dB. A comparison of the S_{11} data for all the operating frequencies is shown in Table 4.

The simulation results for the return loss of the proposed antenna (45 mm × 40 mm) in comparison with the large ground plane antenna (50 mm × 45 mm) and

the wideband antenna that is obtained from the proposed antenna by moving the strip between the slots are shown in Fig. 4 (b). The simulated S_{11} for antenna 1, antenna 3, and the proposed antenna are plotted in Fig. 4 (c). Figure 4 (d) shows the simulated S_{11} for antenna 2 and the proposed antenna, and is shown in Fig. 4 (e) for the proposed antenna that consists of two groups of five slots plotted in comparison with two-, three-, and four-groups of slots, right and left.

Table 4: Simulated and measured S-parameters for the proposed slot antenna

Resonant Freq. (GHz)		S_{11} (dB) at Resonant Freq.		Freq. Range (GHz)	
Sim.	Meas.	Sim.	Meas.	Sim.	Meas.
3.5	3.456	-21.72	-21.17	3.317-3.571	3.295-3.542
4.1	4.028	-29.15	-37.39	3.933-4.193	3.893-4.156
5	4.952	-24.13	-26.14	4.851-5.098	4.708-5.052
6.4	6.516	-33.74	-36.02	5.889-6.6	5.789-6.656
6.8	6.884	-29.48	-45.17	6.6-6.996	6.656-7.035

As presented in Fig. 4 (a) and in Table 2, we can conclude that we have a good agreement between the simulation and measurement results. It is clear that in Fig. 4 (b) the proposed antenna has a good return loss performance in comparison to the other antenna by changing the ground plane to 50 × 45 mm², with no impact on the operating frequency by increasing the ground plane. On the other hand, by shifting the horizontal strips between the slots and leaving 2.5 mm for all four slots ((Ls1r, Ls2r, Ls3r, Ls4r, and Ls1l, Ls2l, Ls3l, Ls4l), the right and left are the same and the largest slot (Ls5r, and Ls5l) with 5 mm remains from the original configuration of the proposed antenna and the wide bandwidth is obtained around the operating frequency of 5.5 GHz with its band (4.796-6.462 GHz) having a 1.666 GHz bandwidth (29.6%).

Figure 4 (c) shows the comparison for the three antenna configurations between antenna 1, proposed antenna, and antenna 3. For antenna 1 and the proposed antenna we see the effect of increasing the left group of slots more than the right group by 0.5 mm and good impedance matching is verified for all the operating frequencies. For antenna 3 by increasing the left slots more than the proposed antenna by 0.5 mm eight operating frequencies are created (3.3, 3.5, 3.9, 4.1, 4.7, 5, 6.1, and 6.8 GHz) and its S_{11} at -14.6, -21, -18.9, -17, -12, -12.1, -24.8, and -26.5 dB, respectively, and the radiating slots are 34.75, 32.75, 29.75, 27.75, 25, 23, 19.75, and 17.75 mm.

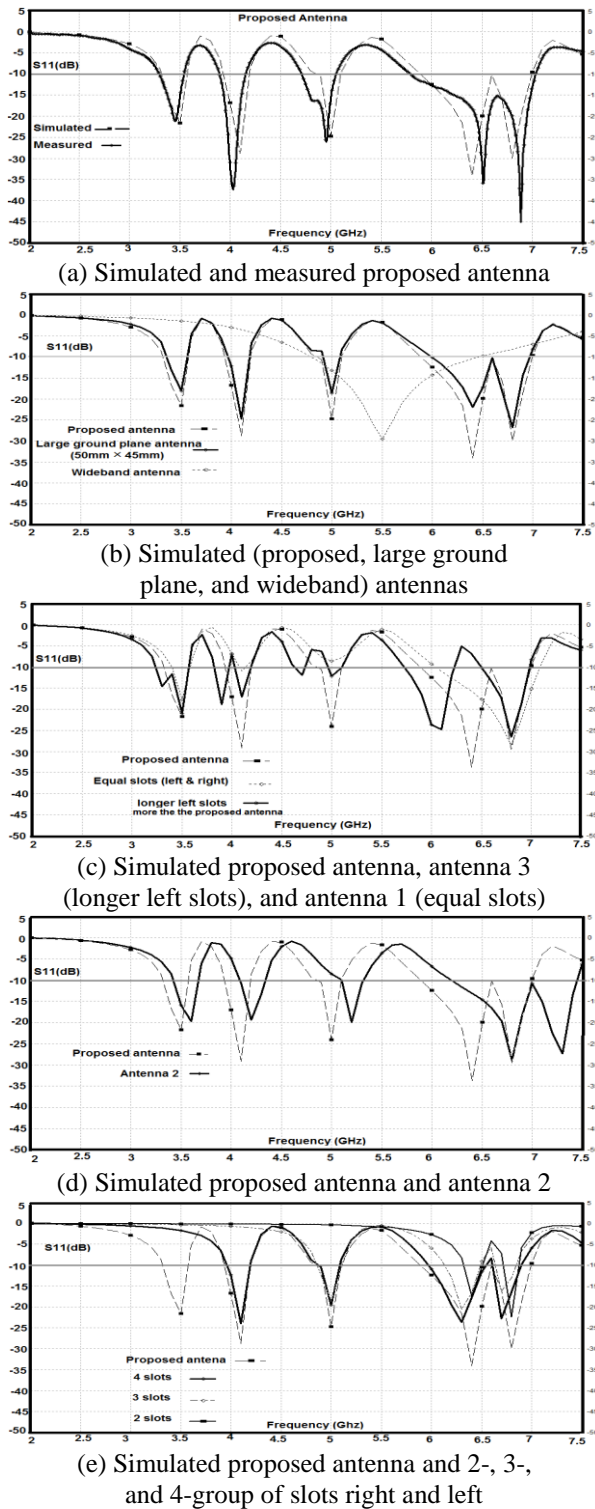


Fig. 4. Return loss of different antenna configurations.

The most useful comparison is shown in Fig. 4 (d), which shows that the proposed antenna with five operating frequencies at 3.5, 4.1, 5, 6.4, and 6.8 GHz and antenna 2 operates at frequencies 3.6, 4.2, 5.2, 6.8, and

7.3 GHz with its S_{11} at -19.8, -19.38, -19.95, -28.9, and -27.35 dB, respectively.

Figure 4 (e) shows the sequence of the proposed design for two groups of two-, three-, and four-slots for right and left in comparison with the proposed antenna.

The simulated peak gains of the proposed planar printed-slot antenna fed by a microstrip line are plotted in Fig. 5. The simulated results of the gain show the values 4.316, 4.334, 4.42, and 5.529 dBi at 3.5, 4.1, 5, and 6.4 GHz, respectively. For a higher frequency of 6.8 GHz (over the bandwidth) the gain was found to have a value of 5.38 dBi.

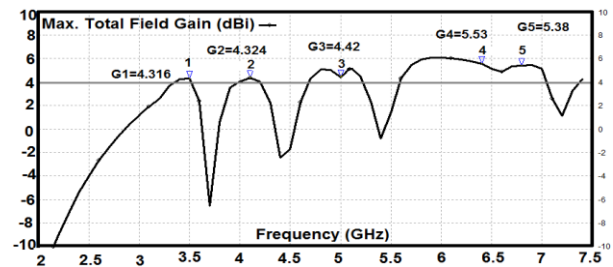


Fig. 5. Simulated gains of the proposed antenna.

The simulated efficiency versus frequency of the proposed planar printed slot antenna is plotted in Fig. 6. The simulated antenna efficiency at the operating frequencies is given by 94.8% at 3.5 GHz, 86.74% at 4.1 GHz, 84.92% at 5 GHz, 91.9% at 6.4 GHz, and finally 90.08% at 6.8 GHz.

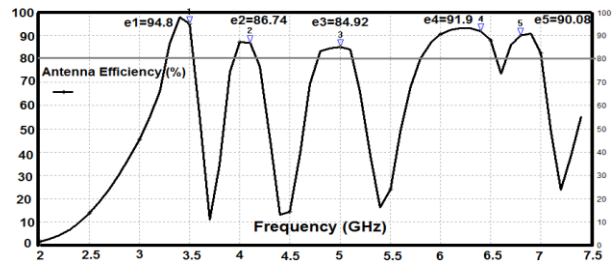


Fig. 6. Simulated efficiency of the proposed antenna.

The maximum directivity measured with the radiation-pattern measurements and the values at the operating frequency in the E-plane (DE) and H-plane (DH) is given in Table 5.

For making a rough estimation about the measured gain, the simulated efficiency is used to calculate the gain based on the measured directivity that is obtained from the radiation-pattern measurements, and it is shown in Table 5.

The radiation-pattern measurements are obtained by using a HP 8650B sweep oscillator (2–26.5 GHz) as a signal generator connected with a standard horn antenna at the corresponding operating frequencies. The

proposed antenna is held on a rotary for covering all the angles of the pattern and the whole system is built inside three covered walls with microwave absorbers. The antenna is connected with a homemade, high-frequency detector and a lock-in amplifier [15], which is interfaced to a personal computer. Therefore, the data can be stored. The simulated and measured far-field radiation patterns (E_{tot}) for the five resonant frequencies (3.5, 4.1, 5, 6.4, and 6.8 GHz) are shown in Fig. 7.

Table 5: The measured directivity (DE, DH) and gain

Freq. (GHz)	3.5	4.1	5	6.4	6.8
DE (dBi)	3.8	4.62	5.31	6.13	5.8
DH (dBi)	3.8	5.68	6.63	6.23	6.13
D (dBi)	3.8	5.182	6.02	6.18	5.97
Gain (dBi)	3.6	4.495	5.11	5.68	5.379

The radiation patterns of the proposed antenna are measured in the anechoic chamber for a verification of the simulated radiation patterns in the E-plane (Y-Z plane) and the H-plane (X-Z plane). It is clear that the radiation patterns in the E-plane for all frequencies under test have a bidirectional pattern; however, the radiation patterns for the H-plane are found to be approximately omnidirectional.

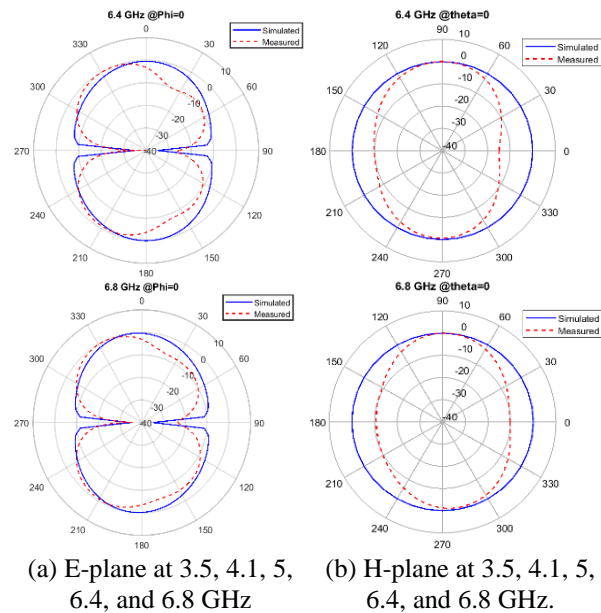
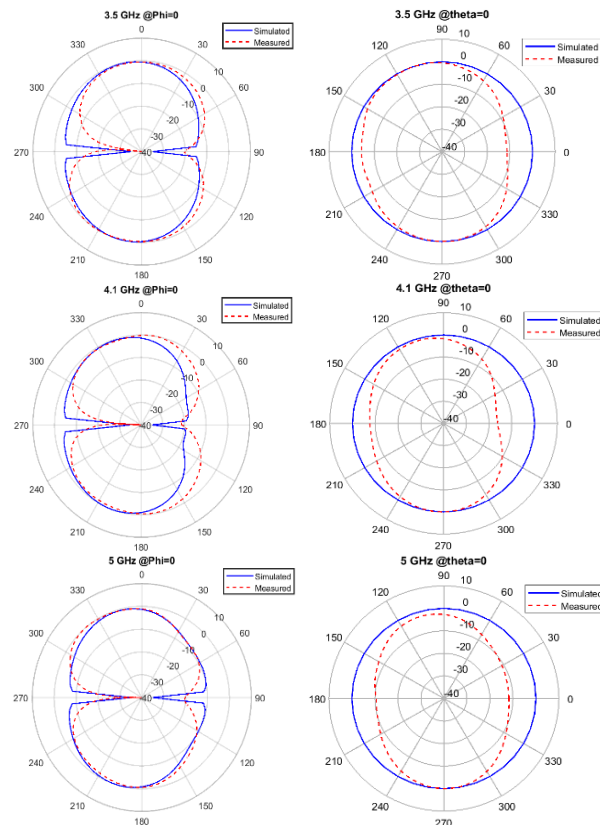


Fig. 7. Simulated and measured radiation patterns of the proposed multiband printed slot antenna.

IV. CONCLUSION

A novel planar-printed slot antenna with slot defects on the ground plane that operates at five bands has been successfully designed and simulated using the IE3D electromagnetic simulator and fabricated using LPKF technology based on a TLT-9 substrate to validate the simulation results. The measured results show good agreement with the simulation results for the return loss and provide a stable radiation pattern for the operating frequencies. The proposed antenna is designed and fabricated on a double-sided PCB, and the obtained results show that the printed-slot antenna can operate effectively at five frequencies with a useful radiation pattern. The impedance bandwidth contains three narrowbands around the operating frequencies (3.5 GHz with (7.23%), 4.1 GHz with (6.53%), and at 5 GHz with (7.05%)) and for the other two integrated in wideband and divided around (6.4 GHz with (13.93%), and 6.8 GHz with (5.54%). The gain varied from 4.316 to 5.529 dBi at the operating frequencies. The design process aimed at the best return losses and fine quality radiation characteristics over all the penta-bands. This makes the antenna design suitable for multiband applications.

ACKNOWLEDGMENT

All the authors thanks to Mr. Bojan Zalar from LPKF Laser & Electronics for fast and precise fabrication of the antenna samples using LPKF ProtoLaser.

REFERENCES

- [1] M. N. Mahmoud and R. Baktur, "A dual band microstrip-fed slot antenna," in *IEEE Transactions on Antennas and Propagation*, vol. 59, no. 5, pp. 1720-1724, May 2011.
- [2] C. Hsieh, T. Chiu, and C. Lai, "Compact dual-band slot antenna at the corner of the ground plane," in *IEEE Transactions on Antennas and Propagation*, vol. 57, no. 10, pp. 3423-3426, Oct. 2009.
- [3] X. L. Bao and M. J. Ammann, "Microstrip-fed dual-frequency annular-slot antenna loaded by split-ring-slot," *IET Microwaves, Antennas & Propagation*, vol. 3, no. 5, pp. 757-764, Aug. 2009.
- [4] O. Amjad, S. W. Munir, S. T. Imeci, and A. O. Ercan, "Design and implementation of dual band microstrip patch antenna for WLAN energy harvesting system," *Applied Computational Electromagnetic Society (ACES) Journal*, vol. 33, no. 7, pp. 746-751, July 2018.
- [5] C. Y. Pan, T. S. Horng, W. S. Chen, and C. H. Huang, "Dual wideband printed monopole antenna for WLAN/WiMAX applications," *IEEE Antennas and Wireless Propagation Letters*, vol. 6, pp. 149-151, 2007.
- [6] M. H. B. Ucar and Y. E. Erdemli, "Triple-band microstripline-fed printed wide-slot antenna for WiMAX/WLAN operations," *Applied Computational Electromagnetic Society (ACES) Journal*, vol. 29, no. 10, pp. 793-800, Oct. 2014.
- [7] F. B. Zarrabi, S. Sharma, Z. Mansouri, and F. Geran, "Triple band microstrip slot antenna for WIMAX/WLAN applications with SRR shape ring," *Fourth International Conference on Advanced Computing & Communication Technologies*, Rohtak, India, pp. 368-371, 2014.
- [8] W. Ren and C. Jiang, "Planar triple-band balance-shaped slot antenna," *Microwave and Optical Technology Letters*, vol. 58, no. 5, pp. 1078-1082, May 2016.
- [9] P. Rakluea, N. Anantrasirichai, K. Janchitrapongvej, and T. Wakabayashi, "Multiband microstrip-fed right angle slot antenna design for wireless communication systems," *ETRI Journal*, vol. 31, no. 3, pp. 271-281, 2009.
- [10] Y. F. Cao, S. W. Cheung, and T. I. Yuk, "A multiband slot antenna for GPS/WiMAX/WLAN systems," *IEEE Transactions on Antennas and Propagation*, vol. 63, no. 3, pp. 952-958, Mar. 2015.
- [11] L. Xiong, P. Gao, and P. Tang, "Quad-band rectangular wide-slot antenna for GPS/WiMAX/WLAN applications," *Progress In Electromagnetics Research C*, vol. 30, pp. 201-211, 2012.
- [12] M. K. Khandelwal, B. K. Kanaujia, and S. Kumar, "Defected ground structure: Fundamentals, analysis, and applications in modern wireless trends," *Hindawi International Journal of Antennas and Propagation*, vol. 2017, 1-23, 2017.
- [13] D. Guha and Y. M. M. Antar, *Microstrip and Printed Antennas: New Trends, Techniques and Applications*. Ch. 12, Wiley, UK, 2011.
- [14] R. Garg, P. Bhartia, I. Bahl, and A. Ittipiboon, *Microstrip Antenna Design Handbook*. Artech House, Norwood, MA, 2001.
- [15] M. Vidmar, "Lock-in receiver with a source up to 12 GHz," <http://lea.hamradio.si/~s53mv/lockin/lockin.html>



Nasr Gad received his B.Sc. and M.Sc. degrees in Electronics from Faculty of Science Ain Shams University, Cairo, Egypt in 2005 and 2012 respectively. Currently, he is pursuing his Ph.D. degree in Electrical Engineering from the University of Ljubljana, Slovenia.

His current research interests include planar printed antenna designing for multiband applications.



Matjaž Vidmar received his B.S.E.E., M.S.E.E., and Ph.D. degrees from University of Ljubljana, Slovenia, in 1980, 1983 and 1992, respectively. His doctoral research concerned the development of a single-frequency GPS ionospheric correction receiver. He currently teaches undergraduate

and postgraduate courses in Electrical Engineering at Ljubljana University, where he is Head of the Radiation and Optics Laboratory (LSO), Department for Electrical Engineering. His current research interests include microwave and high-speed electronics ranging from avionics to optical-fiber communications. Under his leadership, the LSO has developed most of the 10-Gb/s electronics (pulse modulator, clock recovery) used in the Ester (ACTS 063) Project and many 40-Gb/s circuits used in the ATLAS (IST 10626) Project: EAM drivers, transmitter clock distribution, 40- and 80-Gb/s clock-recovery circuits, and 40-Gb/s PMD compensation receiver electronics. He has also developed and built satellite hardware flown in space in 1990 on the Microsat mission and in 2000 on the AMSAT-P3D satellite.